

# Polar Interactions Trump Hydrophobicity in Stabilizing the Self-Inserting Membrane Protein Mystic

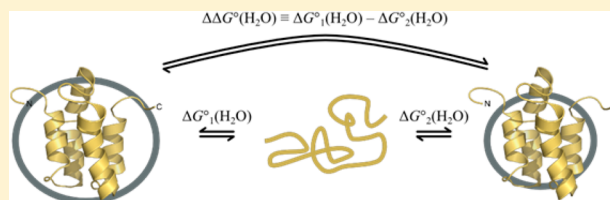
Jana Broecker,<sup>†,‡</sup> Sebastian Fiedler,<sup>†,§</sup> Katharina Gimpl, and Sandro Keller\*

Molecular Biophysics, University of Kaiserslautern, Erwin-Schrödinger-Straße 13, 67663 Kaiserslautern, Germany

**S** Supporting Information

**ABSTRACT:** Canonical integral membrane proteins are attached to lipid bilayers through hydrophobic transmembrane helices, whose topogenesis requires sophisticated insertion machineries. By contrast, membrane proteins that, for evolutionary or functional reasons, cannot rely on these machineries need to resort to driving forces other than hydrophobicity. A striking example is the self-inserting *Bacillus subtilis* protein Mystic, which is involved in biofilm formation and has found

application as a fusion tag supporting the recombinant production and bilayer insertion of other membrane proteins. Although this unusual protein contains numerous polar and charged residues and lacks characteristic membrane-interaction motifs, it is tightly bound to membranes *in vivo* and membrane-mimetic systems *in vitro*. Therefore, we set out to quantify the contributions from polar and nonpolar interactions to the coupled folding and insertion of Mystic. To this end, we defined conditions under which the protein can be unfolded completely and reversibly from various detergent micelles by urea in a two-state equilibrium and where the unfolded state is independent of the detergent used for solubilizing the folded state. This enabled equilibrium unfolding experiments previously used for soluble and  $\beta$ -barrel membrane proteins, revealing that polar interactions with ionic and zwitterionic headgroups and, presumably, the interfacial dipole potential stabilize the protein much more efficiently than nonpolar interactions with the micelle core. These findings unveil the forces that allow a protein to tightly interact with a membrane-mimetic environment without major hydrophobic contributions and rationalize the differential suitability of detergents for the extraction and solubilization of Mystic-tagged membrane proteins.



## INTRODUCTION

Most integral membrane proteins are anchored to lipid bilayers by virtue of transmembrane segments rich in nonpolar, hydrophobic amino acid residues. Their pronounced hydrophobicity is a distinguishing feature of integral membrane proteins that has long formed the basis of hydrophobicity plots<sup>1</sup> used to identify such proteins and predict their topologies. Recently, these tasks have been aided by refined<sup>2,3</sup> and “biological”<sup>4</sup> hydrophobicity scales, culminating in a quantitative link between first-principle physical chemistry and membrane-protein topogenesis in cellular translocons.<sup>5</sup> By contrast, nonhydrophobic contacts among polar groups are believed to make a negligible or even unfavorable contribution to the lipid association of integral membrane proteins,<sup>6</sup> although they are crucial for specific interactions among transmembrane helices<sup>7</sup> and for the reversible adsorption of peripheral membrane proteins.<sup>8</sup>

However, a growing number of observations defy the canonical distinction<sup>9</sup> between integral membrane proteins hydrophobically tethered to lipids and peripheral membrane proteins associated only loosely. This is particularly true for proteins that need to insert into membranes without relying on elaborate machineries of chaperones and translocons essential for handling hydrophobic membrane proteins.<sup>10</sup> For instance, the membrane pore of staphylococcal  $\alpha$ -hemolysin remains functional after truncation of large parts of its transmembrane

domain,<sup>11</sup> and amphipathic peptides rich in cationic and anionic residues may form membrane-spanning charge zippers.<sup>12</sup> An even more drastic example is Mystic,<sup>13</sup> an unusual *Bacillus subtilis* protein that is essential for biofilm formation<sup>14</sup> and is biotechnologically exploited as a fusion tag to support the membrane targeting, insertion, and detergent-mediated solubilization of other membrane proteins.<sup>13,15–29</sup> Mystic comprises 110 residues that are arranged into a four-helix bundle exposing numerous polar and charged residues (Supporting Information Figure S1), which is incompatible with a transmembrane topology. Having a predicted pI of 4.5, a net charge at pH 7.0 of  $-12$ , and a mean hydrophobicity on the normalized Kyte/Doolittle scale<sup>1</sup> of 0.43, Mystic should be more hydrophilic than typical soluble globular proteins and might even be expected to be an intrinsically disordered protein.<sup>30</sup> In spite of these hydrophilic characteristics, Mystic tightly associates with membranes *in vivo*<sup>13,31</sup> and membrane-mimetic systems *in vitro*,<sup>13,32–34</sup> thus qualifying, by operational definition,<sup>9</sup> as an integral membrane protein. During cell-free production, the yield and fold of Mystic are modulated by both lipid headgroup chemistry as well as acyl chain length and saturation.<sup>33</sup> In line with this, NMR experiments<sup>13,34</sup> have confirmed that the protein is embedded within detergent

Received: June 27, 2014

Published: September 1, 2014

micelles, and the solubilization behavior of Mystic fusion constructs strongly depends on both detergent headgroup and tail properties,<sup>16,25</sup> although it contrasts markedly with the detergent preferences of most other membrane proteins (see Discussion).

The unexpected but demonstrably firm association of Mystic with lipid bilayers and detergent micelles indicates that this hydrophilic protein eludes our current understanding of membrane-protein folding and stability. Here, we dissect the determinants governing its conformational stability in and affinity for micellar environments and rationalize the differential suitability of detergents for solubilizing Mystic fusion proteins during the recombinant production of other membrane proteins. To this end, we define conditions under which Mystic can be unfolded completely and reversibly with the aid of the chemical denaturant urea and demonstrate that the unfolded polypeptide chain is dissociated from micelles and largely devoid of secondary structure, thus representing a reference state for a comparison of protein stability among different membrane mimetics. Together with the rich headgroup chemistry offered by detergents (Supporting Information Figure S2), these features are exploited to quantify the contributions from polar and nonpolar interactions to the conformational stability of Mystic. Although the latter depends on hydrophobic micelle thickness, as expected for a membrane-embedded protein, it reaches maximum values only in the presence of ionic and zwitterionic headgroups. These findings establish a paradigm in which polar headgroup interactions rather than hydrophobic contacts provide the dominant forces driving the folding of a hydrophilic protein into a membrane-mimetic environment.

## RESULTS

**Ionic and Zwitterionic Detergent Headgroups Stabilize Mystic.** The solution NMR structure<sup>13</sup> of Mystic was solved in the zwitterionic detergent lauryldimethylamine *N*-oxide (LDAO). When titrated with urea, LDAO-solubilized Mystic loses some helical secondary structure but is resistant against complete unfolding.<sup>34</sup> This was reflected in circular dichroism (CD) spectra, which retained helical features in the form of two intense minima at 222 nm and below 210 nm even in the presence of 6.3 M urea (Figure 1a). However, stepwise extraction of LDAO by complexation with methylated  $\beta$ -cyclodextrin (M $\beta$ CD) under such denaturing conditions caused a sharp decline in helicity at the critical micellar concentration (CMC) of the detergent, as borne out by a steep decrease in the intensity of the CD signal at 222 nm (Figure 1a, Supporting Information Figures S3 and S4). Thus, the protective effect of strong interactions with the LDAO headgroup<sup>34</sup> depends on a micellar environment.

On the premise that modulating interactions with detergent headgroups may be key to rendering Mystic amenable to complete unfolding in the presence of micelles, we screened a set of chemically diverse dodecyl detergents carrying anionic, cationic, zwitterionic, or nonionic headgroups (Figure 1b, Supporting Information Figure S2). To make sure that unfolding was caused by protein destabilization rather than micelle dissolution with increasing urea concentration,<sup>35</sup> the concentration of each detergent was adjusted such that at least 5 mM detergent was present in micellar form (Supporting Information Figures S5–S8, Table S1).

The anionic detergent sodium dodecyl sulfate (SDS) is considered “harsh” because it denatures most soluble and

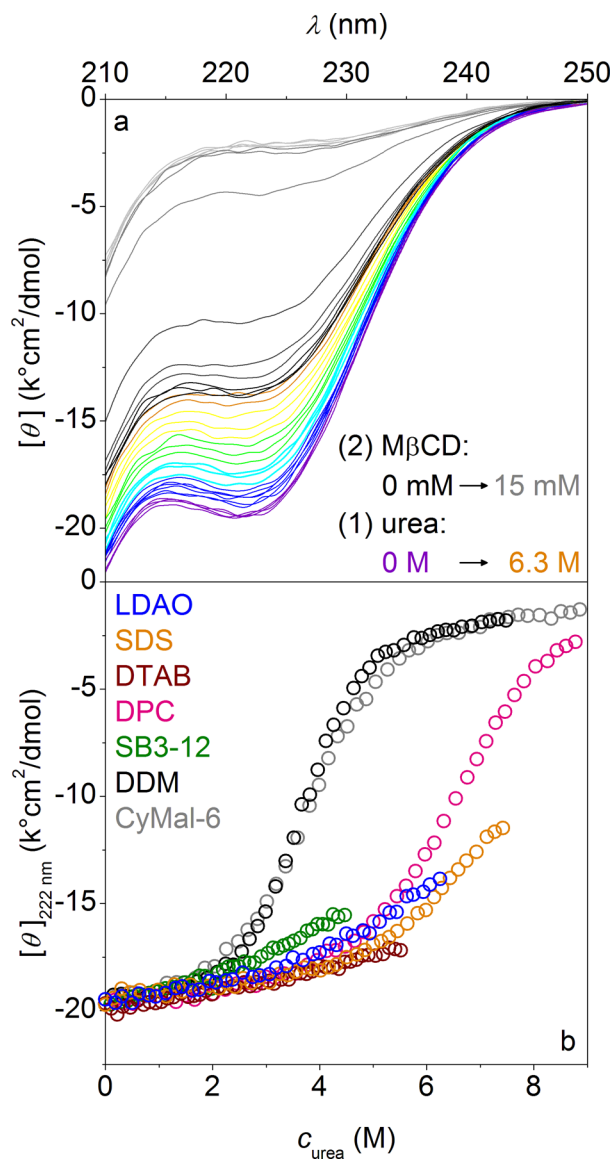


**Figure 1.** Influence of detergent headgroup properties on urea-induced unfolding of Mystic. (a) CD spectra of 20  $\mu$ M Mystic in 12 mM LDAO sequentially titrated with urea and M $\beta$ CD. First, urea concentration was raised from 0 to 6.3 M in the presence of LDAO micelles. Then, in the presence of 6.3 M urea, M $\beta$ CD concentration was increased from 0 to 15 mM to dissolve micelles. (b) Unfolding isotherms of 20  $\mu$ M Mystic solubilized in 12 mM LDAO, 66.8 mM SDS, 47.2 mM DTAB, 19.7 mM SB3-12, 12.1 mM DPC, 6.08 mM DDM, or 9.09 mM CyMal-6. LDAO, SDS, DTAB, and SB3-12 are insoluble at high urea concentrations.  $\lambda$ , wavelength;  $[\theta]$ , molar residual ellipticity;  $c_{\text{urea}}$ , urea concentration; 50 mM Tris, 50 mM NaCl, pH 7.4, 20  $^{\circ}$ C.

membrane proteins. However, denaturation is different from unfolding,<sup>36</sup> as SDS can even induce non-native secondary structure in a process dubbed “reconstructive denaturation”.<sup>37</sup> Indeed, we found SDS as well as cationic *n*-dodecyltrimethylammonium bromide (DTAB) and zwitterionic *N*-dodecyl-*N,N*-dimethyl-3-ammonio-1-propanesulfonate (SB3-12) to behave similarly to LDAO in protecting Mystic against complete unfolding (Figure 1b). In zwitterionic *n*-dodecylphosphocholine (DPC), in which Mystic assumes the same structure as in LDAO,<sup>32</sup> the protein exhibited an unstructured conformation at urea concentrations >8 M. The unfolding isotherm followed

a sigmoidal shape with a transition midpoint,  $c_M$ , at  $\sim 7$  M urea, resulting in a well-defined pretransition baseline and an ill-defined post-transition baseline. By contrast, the two nonionic, "mild" detergents *n*-dodecyl- $\beta$ -D-maltoside (DDM) and 6-cyclohexyl-1-hexyl- $\beta$ -D-maltoside (CyMal-6) stabilized the protein much less effectively, yielding unfolding isotherms with  $c_M \approx 4$  M urea and well-defined post-transition baselines indicative of a largely unstructured state at  $>6$  M urea.

**Mistic Is a Reversible Two-State Folder in Alkyl Maltosides.** To examine if Mistic is a two-state folder when solubilized in DDM, we monitored unfolding using both CD and intrinsic Trp fluorescence (FL) emission as two independent spectroscopic probes reporting on, respectively, global secondary structure and the environment of the lone Trp residue at position 13. CD spectra corroborated that the protein was helical in the absence of denaturant but unfolded at  $>7$  M urea (Figure 2a), which was paralleled by a red shift of FL emission, indicating an increase in the local dielectric constant and, thus, solvent exposure of Trp13 (Figure 2b). Refolding of unfolded Mistic yielded spectra identical to those obtained using protein freshly prepared under native conditions (Supporting Information Figure S9), and isotherms constructed by plotting the ellipticity at 222 nm or the wavelength of maximum FL intensity,  $\lambda_{\max}$  versus urea concentration did not depend on whether the protein was initially folded or unfolded (Figure 2c/d).

A position–width plot<sup>38,39</sup> depicting the full spectral width at half-maximum FL emission intensity,  $\Gamma$ , as a function of  $\lambda_{\max}$  confirmed both two-state folding and reversibility (Figure 2e). We compared the spectral properties of Mistic in DDM obtained over the entire urea concentration range to those of *N*-acetyl Trp amide (NATA) dissolved in various mixtures of water and dioxane, which represent homogeneous populations of indole chromophores exposed to different polarities. Under native or strongly denaturing conditions, the spectral properties of Mistic were close to the NATA baseline, indicating homogeneous Trp populations in both the folded and unfolded states. By contrast, FL spectra acquired at intermediate urea concentrations followed an arc-shaped bend as predicted for a two-state folder.<sup>39</sup>

To explore if the CD and FL results are consistent with each other also at a quantitative level, we first analyzed data from either method individually in terms of a two-state equilibrium. We applied the linear extrapolation model<sup>40,41</sup> to determine the Gibbs free-energy change upon unfolding in the absence of denaturant,  $\Delta G^\circ(\text{H}_2\text{O})$ , and the  $m$ -value, which is the negative derivative of unfolding free energy with respect to urea concentration,  $m \equiv -\partial\Delta G^\circ/\partial c_{\text{urea}}$ . This was followed by a global fit in which all isotherms from CD and FL experiments shared the same values of  $\Delta G^\circ(\text{H}_2\text{O})$  and  $m$  (Supporting Information Figure S10). The best-fit values did not depend on the spectroscopic signal or wavelength (Supporting Information Table S2), confirming that DDM-solubilized Mistic is a two-state folder. The same set of experiments demonstrated fully reversible two-state folding also when the shorter-chain analogue nonyl maltoside (NM) was used as solubilizing detergent (Supporting Information Figure S11).

**The Unfolded State Is Dissociated from Micelles.** To test if the folded and unfolded states depend on detergent in micellar form, we used M $\beta$ CD to complex DDM and reduce its free concentration below the CMC (Supporting Information Figure S4). While micelle dissolution caused a loss in secondary structure under native conditions and throughout the transition

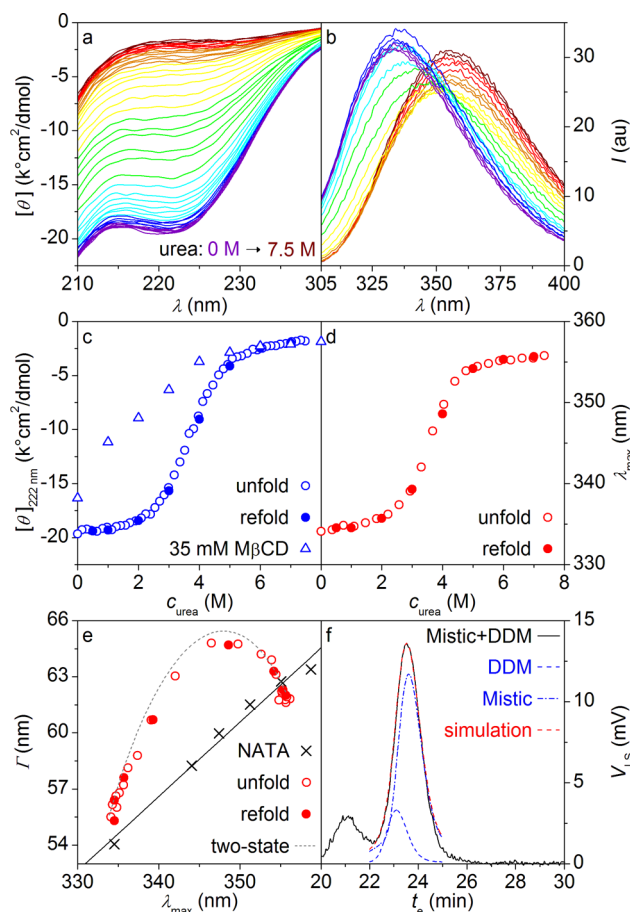


**Figure 2.** Reversible two-state unfolding of Mistic in DDM. (a) CD and (b) FL emission spectra of 20  $\mu\text{M}$  Mistic in 6.08 mM DDM as functions of urea concentration. Trp FL was excited at 295 nm. (c) CD and (d) FL unfolding and refolding isotherms. CD unfolding isotherms were obtained also upon dissolution of micelles by addition of 35 mM M $\beta$ CD, which lowered the DDM concentration to  $<2.5$   $\mu\text{M}$ , as calculated from the DDM/M $\beta$ CD dissociation constant (Supporting Information Figure S4d). (e) Position–width plot. NATA data obtained in mixtures of water and dioxane were fitted to a straight line; simulated two-state data were derived from linear combinations of experimental spectra of folded and unfolded states. (f) SEC of 78  $\mu\text{M}$  Mistic and 6.08 mM DDM in the presence of 6 M urea as monitored by right-angle light scattering. The simulated chromatogram represents the sum of the scattering contributions from detergent-free Mistic and protein-free DDM micelles (Supporting Information Figure S13).  $\lambda$ , wavelength;  $[\theta]$ , molar residual ellipticity;  $I$ , FL intensity;  $c_{\text{urea}}$ , urea concentration;  $\lambda_{\max}$ , wavelength of maximum FL intensity;  $\Gamma$ , full width of FL emission spectrum at half-maximum intensity;  $t_e$ , elution time;  $V_{\text{LS}}$ , voltage of 90° light scattering detector; 50 mM Tris, 50 mM NaCl, pH 7.4, 20 °C.

range, it had no effect at  $>6$  M urea (Figure 2c). Similarly, the absence of micellar detergent resulted in protein aggregation under native conditions but not in the presence of high urea concentrations (Supporting Information Figure S12). Size exclusion chromatography (SEC) coupled to absorbance, light scattering, and refractive index detection showed that, under denaturing conditions, detergent-free Mistic and protein-free DDM micelles eluted as two independent species (Figure 2f, Supporting Information Figure S13). Hence, micelles are crucial for the structural integrity of folded Mistic but do not affect the unfolded state. Since this was confirmed also for NM (Supporting Information Figure S13), the



unfolded polypeptide chain may serve as a reference state that is independent of the detergent used for solubilizing the folded state, paving the way for a quantitative comparison of protein stability as a function of detergent properties.

**Unfolding Behavior Depends on Hydrophobic Micelle Thickness.** To quantify the contributions of nonpolar interactions to the conformational stability of Mystic, we unfolded the protein from micelles composed of alkyl maltosides varying in chain length from 8 to 14 carbon atoms. Irrespective of the detergent used, Mystic exhibited a helical content of  $\sim 60\%$  in the absence of urea but was virtually devoid of secondary structure at high urea concentrations (Supporting Information Figures S14 and S15), which is in excellent agreement with the NMR structures of the folded<sup>13</sup> and unfolded<sup>34</sup> states, respectively. Although the transition midpoint was always close to 3.5–4.0 M urea, the shape of the unfolding isotherm depended on chain length (Figure 3), as a flat transition observed for short-chain detergents gradually gave way to a sigmoidal isotherm with well-defined pre- and post-transition baselines as the chain became longer. Global analysis of triplicate unfolding isotherms (Supporting Information Figure S16) revealed that, as the chain was extended from 9 to 14 carbon atoms,  $\Delta G^\circ(\text{H}_2\text{O})$  increased from 8.1 to 17.1 kJ/mol (Figure 4a), while  $m$  increased from 2.0 to 5.0 kJ/(mol M) (Figure 4b). Both parameter values experienced large changes for short chains and leveled off at higher chain lengths, which tallied with an asymptotic decrease in the  $\lambda_{\text{max}}$  values of the folded state from 338 nm in OM to 333 nm in TetraDM (Supporting Information Figure S14).

**Hydrophobic and Polar Interactions Contribute to Stability.** To explore the influence of both chain and headgroup properties, we unfolded Mystic from various other nonionic detergents (Supporting Information Figures S17 and S18). Like DDM, CyMal-6 is made up of a maltose headgroup and a dodecyl chain, which, however, features a terminal cyclohexyl function (Supporting Information Figure S2). In comparison with DDM, the resulting decrease in micelle thickness diminished the stability of Mystic in the absence of denaturant by 2.3 kJ/mol (Figure 4a) and, concomitantly, decreased its susceptibility to urea in terms of the  $m$ -value by 0.8 kJ/(mol M) (Figure 4b), leading to a very similar value of  $c_M = 3.8$  M urea. Conversely, reducing the size of the sugar headgroup through replacement of NM by its glucose-headed counterpart nonyl glucoside (NG) stabilized the protein by 2.7 kJ/mol (Figure 4a) and increased  $m$  by 0.4 kJ/(mol M) (Figure 4b), again yielding only moderate changes in  $c_M$ . The only means of breaking this compensatory correlation between  $\Delta G^\circ(\text{H}_2\text{O})$  and  $m$  was through the introduction of (zwitter)-ionic headgroups (Figure 1b). In DPC (Supporting Information Figure S19),  $\Delta G^\circ(\text{H}_2\text{O})$  amounted to 18.5 kJ/mol, which was the greatest stability measured among all detergents for which reliable quantification was possible (Figure 4a, Supporting Information Table S3). In contrast with the situation encountered for nonionic detergents, this enhanced stability in the absence of denaturant was not offset by an increase in  $m$ , which amounted to only 2.6 kJ/(mol M) (Figure 4b), resulting in a high value of  $c_M = 7.1$  M urea (Figure 1b).

## DISCUSSION

**Headgroup Interactions Stabilize a Hydrophilic Membrane Protein.** Owing to its unusual hydrophilicity, Mystic can be unfolded from micelles in a complete and reversible manner (Figures 1–3), which sets it apart from

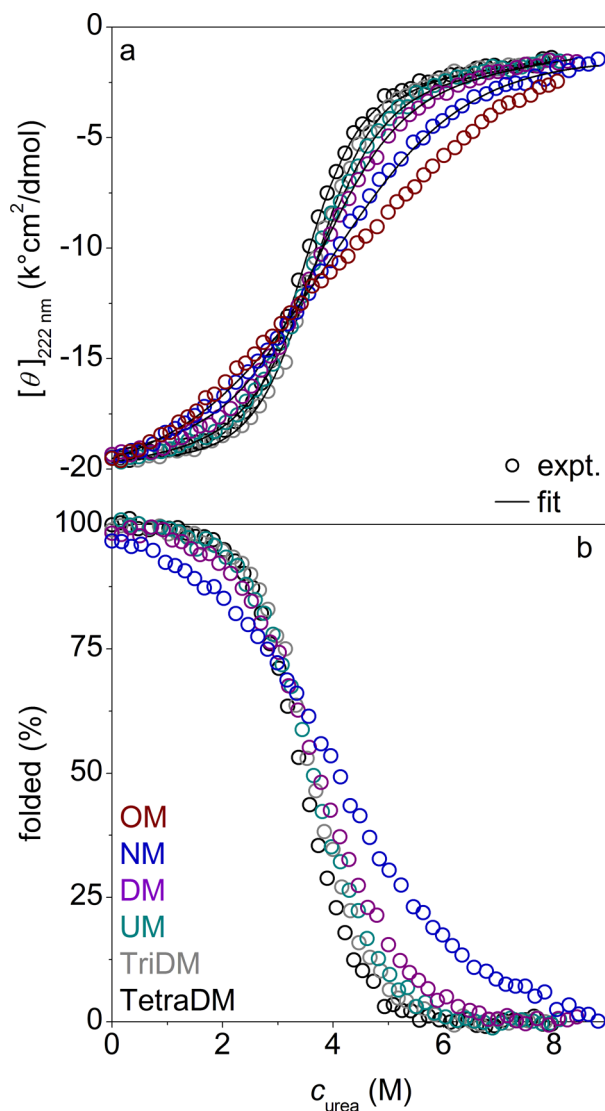


**Figure 3.** Urea-induced unfolding of Mystic in a homologous series of alkyl maltosides having chain lengths of 8–14 carbon atoms. (a) Unfolding isotherms and (b) normalized unfolding isotherms of 20  $\mu\text{M}$  Mystic in the presence of 80.9 mM octyl maltoside (OM), 29.6 mM NM, 13.8 mM decyl maltoside (DM), 8.24 mM undecyl maltoside (UM), 5.0 mM tridecyl maltoside (TriDM), or 5.0 mM tetradecyl maltoside (TetraDM).  $[\theta]_{222\text{ nm}}$ , molar residual ellipticity at 222 nm;  $c_{\text{urea}}$ , urea concentration; 50 mM Tris, 50 mM NaCl, pH 7.4, 20  $^\circ\text{C}$ .

canonical helical-bundle transmembrane proteins.<sup>36,41–43</sup> As borne out by the  $\Delta G^\circ(\text{H}_2\text{O})$  and  $m$ -values, respectively, both the conformational stability of Mystic in the absence of denaturant (Figure 4a) as well as its susceptibility to urea (Figure 4b) depend on the thickness of the hydrophobic micelle core. For water-soluble<sup>44</sup> and  $\beta$ -barrel membrane proteins,<sup>45</sup> the  $m$ -value is a measure of the change in solvent-accessible surface area accompanying protein unfolding. Along these lines, and notwithstanding additional considerations bearing on protein-stability determination in a micellar environment (Supporting Discussion), our  $m$ -values indicate deeper penetration of Mystic into the core and, thus, better shielding from water as the detergent chain becomes longer. This is corroborated by a concomitant decrease in  $\lambda_{\text{max}}$  of the folded state (Supporting Information Figure S14), reflecting a

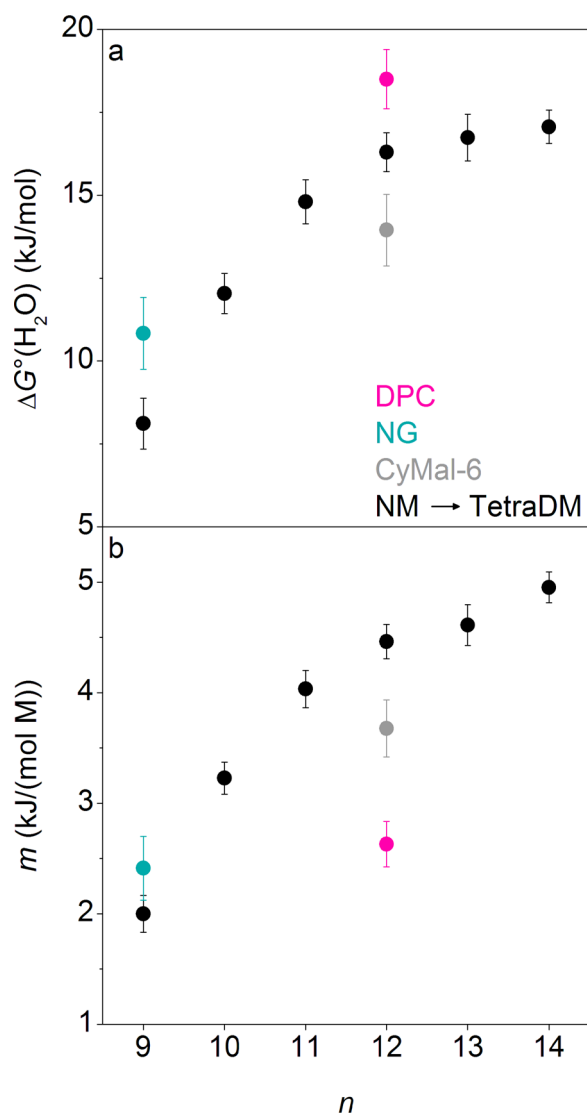


**Figure 4.** Thermodynamic parameters characterizing urea-induced unfolding of Mystic. (a) Conformational stability under native conditions. (b) Influence of urea on conformational stability. Error bars give 68.3% confidence intervals. Results for OM have large uncertainties and are not shown.  $n$ , number of carbon atoms in the alkyl chain;  $\Delta G^\circ(\text{H}_2\text{O})$ , standard molar Gibbs free-energy change upon unfolding in the absence of denaturant;  $m$ ,  $m$ -value.

reduction in the dielectric constant around Trp13. The correlation between protein burial in nonionic micelles and native-state stability (Figure 5a) therefore implies a contribution from hydrophobic shielding to conformational stability.

Even under optimum conditions, however, the stability of Mystic in nonionic detergents is limited, leveling off at  $\sim 17$  kJ/mol (Figure 4a). Further stabilization is achieved only by detergents carrying (zwitter)ionic headgroups. Among the latter, DPC is the only one in which Mystic can be unfolded to the same extent as in nonionic detergents (Figure 1b). Inspection of  $m$  (Figure 4b) and  $\lambda_{\text{max}}$  (Supporting Information Figure S14) reveals that DPC is much less effective than DDM in shielding Mystic from the aqueous solvent, although both detergents carry a dodecyl chain. This is explained by more extensive hydration of and deeper water penetration into the headgroup region of a zwitterionic DPC micelle.<sup>46</sup> Although, as gauged by the above two parameters, DPC performs on par

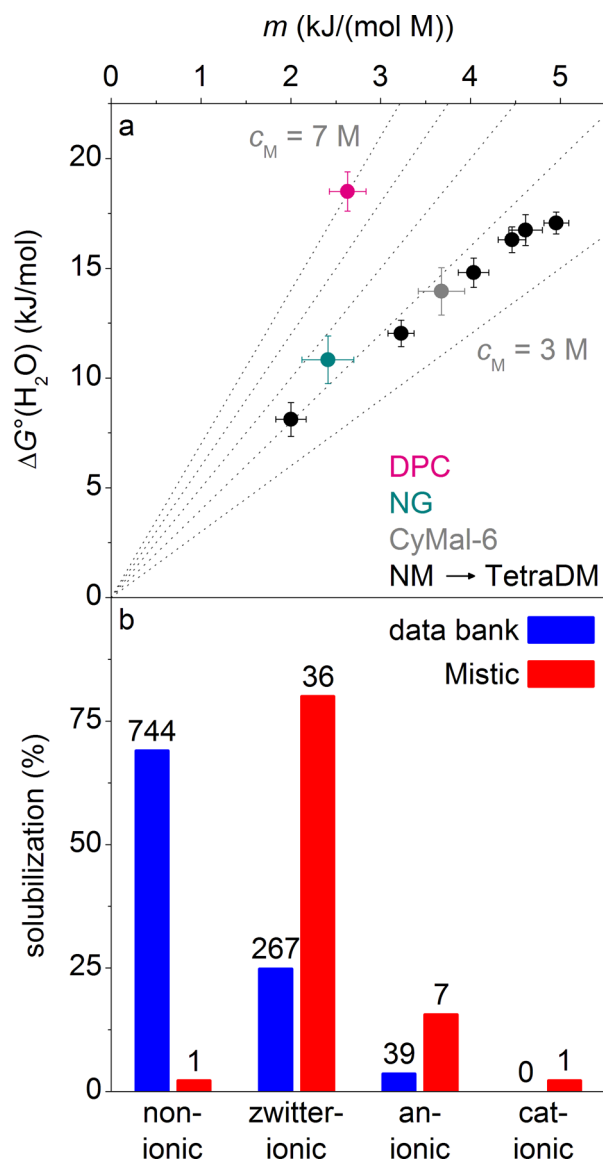


**Figure 5.** Correlation between conformational stability and solubilization behavior of Mystic. (a) Correlation between stability under native conditions and influence of urea on stability. Error bars give 68.3% confidence intervals. Dotted lines indicate constant values of the transition midpoint in the range  $3 \text{ M} \leq c_M \leq 7 \text{ M}$ . (b) Comparison of 45 Mystic fusion proteins solubilized from *Escherichia coli* membranes after recombinant production<sup>13,15,17–21,23,25,27,28</sup> against 1078 integral membrane proteins listed in the membrane protein data bank.<sup>48</sup> Absolute numbers are given above each bar.  $\Delta G^\circ(\text{H}_2\text{O})$ , standard molar Gibbs free-energy change upon unfolding in the absence of denaturant;  $m$ ,  $m$ -value.

with the shorter-chain nonionic detergents NM or DM in protecting the folded protein from solvent access, it provides much greater stability. Taking the average  $\Delta G^\circ(\text{H}_2\text{O})$  value in NM and DM ( $\sim 10$  kJ/mol) as an upper bound on the hydrophobic contribution to stability in DPC ( $\sim 19$  kJ/mol), we arrive at an additional stabilization of  $\sim 9$  kJ/mol due to polar interactions between Mystic and the phosphocholine headgroup. Other (zwitter)ionic headgroups stabilize the protein even more dramatically, to an extent that it can no longer be unfolded even at the highest accessible urea concentrations (Figure 1). Persistent detergent contacts and resistance against unfolding are common among membrane

proteins;<sup>41</sup> in the case of Mystic, however, they do not result from detergent binding to hydrophobic clusters<sup>47</sup> but are mediated by strong interactions with detergent headgroups. In the case of LDAO, such polar contacts prevent urea from accessing the polypeptide backbone and unraveling large parts of the third and fourth helical segments of Mystic.<sup>34</sup>

**Coupled Folding and Insertion into the Interface.** The strength of membrane or micelle insertion is largely determined by competing dehydration free-energy terms,<sup>49</sup> which are favorable for nonpolar side chains and unfavorable for polar side chains and the polypeptide backbone. Under all conditions probed in this study, the folding of Mystic is strictly coupled to its insertion into micelles (Figure 2f, Supporting Information Figure S13). In other words, Mystic exists either as a soluble unstructured polypeptide or as a micelle-bound folded protein. The absence of a micelle-bound but unstructured state is straightforward to explain, as the Wimley–White interfacial hydrophobicity scale<sup>50</sup> predicts a highly endergonic value of  $\sim 200$  kJ/mol for the hypothetical transfer of unfolded Mystic from water into a phosphocholine headgroup layer. By contrast, the absence of a soluble folded state is more interesting, as it indicates that, outside a membrane-mimetic environment, the changes in intramolecular and hydration interactions accompanying folding are insufficient to stabilize the native fold.

Thus, the question boils down to pinpointing the additional interactions Mystic engages in only when it is both folded and inserted. As discussed above, hydrophobic burial in the micelle core of nonpolar residues not shielded through intramolecular interactions upon folding is at play but cannot explain the dependence of  $\Delta G^\circ(\text{H}_2\text{O})$  on headgroup properties (Supporting Information Figure S2). Intramolecular salt bridges, dispersion forces, and hydrogen bonds are unlikely to make a decisive difference, as their contributions to protein stability appear to be similar in aqueous and membranous environments.<sup>36</sup> Strikingly, Mystic possesses no fewer than 8 Asp and 17 Glu residues, almost all of which are highly conserved among all orthologs occurring in various *Bacillus* species.<sup>15</sup> This points to a crucial function of anionic residues and their positioning on the surface of the helical bundle (Supporting Information Figure S1), even if  $\text{p}K_a$  shifts in a nonpolar environment may cause partial neutralization.<sup>51</sup> The importance of these residues is also supported by the observation that truncated or mutated Mystic variants, some of which exist in both soluble but oligomeric or aggregated as well as monomeric membrane-bound forms,<sup>52</sup> exhibit markedly impaired membrane-insertion capabilities.<sup>19</sup> However, purely Coulombic attraction toward the headgroup layer, which promotes the folding and insertion into anionic lipid bilayers of cationic peptides and proteins,<sup>8</sup> can be dismissed here because cationic, anionic, as well as zwitterionic detergents all strongly stabilize Mystic (Figure 1b).

**A Role for the Interfacial Dipole Potential in Stabilizing an Anionic Membrane Protein.** Sequence-based hydrophobicity scales do not account for the fact that dehydration free energies and other polar interactions strongly depend on context.<sup>53,54</sup> For example, the highly unfavorable dehydration free energies of free Glu and Asp turn favorable when these residues are placed in the context of a soluble protein with net positive charge because the orientational distribution of hydrating water layers results in repulsive interactions of the water dipoles with anionic protein moieties.<sup>55</sup> Analogously, zwitterionic phospholipid bilayers possess a pronounced interfacial dipole potential due to the

orientations of acyl carbonyl groups and water molecules hydrating the headgroups, with positive values of up to +300 mV inside the nonpolar membrane core.<sup>56</sup> This is recapitulated in cationic and zwitterionic micelles<sup>57</sup> and, somewhat unexpectedly, even in anionic ones. In the case of SDS, for instance, the orientation of hydration-water dipoles overrules the negative charge of the headgroup and thus dictates the direction of the net dipole moment across the interface.<sup>58</sup> Therefore, even marginally hydrophobic and poorly polarizable anions such as acetate reveal a favorable Gibbs free-energy change of  $-0.5$  kJ/mol upon transfer into the micellar headgroup region.<sup>57</sup> The membrane dipole potential has long been suspected to affect membrane-protein stability,<sup>59</sup> and recent experiments implicate it in governing the coupled folding and bilayer insertion of an anionic  $\beta$ -barrel membrane protein.<sup>60</sup>

In light of this, we speculate that the conserved positioning of anionic groups on the surface of Mystic<sup>15</sup> serves to exploit the interfacial dipole potential. Results from computational approaches are in accord with this hypothesis. Simple models representing a lipid membrane as a headgroup-free nonpolar slab<sup>61</sup> predict only shallow insertion of a few residues (<http://opm.phar.umich.edu/protein.php?search=1ygm>), as expected on the basis of Mystic's overall hydrophilic characteristics. By contrast, coarse-grained molecular dynamics simulations,<sup>62</sup> which implicitly account for the interfacial dipole potential, headgroup interactions, and bilayer deformability, suggest a radically different picture in which Mystic is immersed into the membrane with its helices lying parallel to the bilayer plane (<http://sbcb.bioch.ox.ac.uk/cgdb/simtable.php?pdb=1ygm>). Together with local membrane perturbation, particularly bilayer thinning, this highly unconventional topology would allow polar side chains to sense the positive dipole potential within the membrane and to interact with lipid headgroups and water along the interfacial regions of both leaflets. Although the detailed topology of Mystic remains to be resolved, the present results would be in agreement with such a scenario enabling the burial of nonpolar residues without excessive dehydration of polar moieties.

**Thermodynamic Stability Rationalizes Membrane Targeting and Protein Solubilization.** Mystic appears to fold into membranes in a translocon-independent manner,<sup>13</sup> which has been taken as an indication that its *in vivo* function consists in aiding the membrane targeting of YugO, a putative  $\text{K}^+$  channel encoded in the same bicistronic operon.<sup>14</sup> Since the two genes are frame-shifted by one base, they are expressed as two separate polypeptide chains; thus, Mystic must fulfill its *in vivo* function as a protein as used in the present study rather than as an N-terminal domain of YugO. Release of  $\text{K}^+$  triggers transition of *B. subtilis* from a motile, solitary state into a biofilm,<sup>63</sup> and the interplay of Mystic and YugO has indeed been shown to be essential for derepressing biofilm formation.<sup>14</sup> Although mechanistic details remain to be elucidated, thermodynamic data provide a quantitative basis for understanding the membrane-targeting function of Mystic and, possibly, other membrane-inserting proteins that bypass the translocon,<sup>10</sup> as headgroup-dependent conformational stabilities (Figure 4a) demonstrate how a hydrophilic protein can avidly associate with lipids in the absence of major hydrophobic driving forces.

Mystic has hitherto been used as an N-terminal fusion tag to improve the recombinant production of 45 integral membrane proteins.<sup>13,15–29</sup> Most of these studies relied on detergents to



extract the fusion protein of interest from the host membrane. In 11 reports,<sup>13,15,17–21,23,25,27,28</sup> a total of 23 detergents were screened for their solubilization efficiencies (Supporting Information Table S4). Systematic solubilization trials<sup>25</sup> using a homologous series of phosphocholine detergents showed that protein yield increases with chain length, mirroring the dependence of conformational stability on micelle thickness (Figure 4a). More strikingly, while 10<sup>13,15,17–23,25,28</sup> out of 12 (zwitter)ionic detergents were able to extract the fusion protein, only one<sup>20</sup> out of 10 nonionic detergents proved suitable for this purpose. Thus, (zwitter)ionic headgroups not only afford highest stability (Figure 1b) but also fare best in solubilizing Mystic fusion proteins (Figure 5b). This is in stark contrast with the picture obtained for other membrane proteins, where (zwitter)ionic detergents are often avoided because of their denaturing effect, although many of them possess properties favorable for structural investigations. Statistical analysis of a broad range of membrane proteins for which high-resolution structures are available<sup>48</sup> indeed reveals a strong preference for nonionic detergents over zwitterionic and, even more clearly, ionic ones (Figure 5b).

A causal relationship between detergent-dependent *in vitro* stability and extraction efficiency appears plausible in view of the fact that membrane proteins, particularly at the high densities typical of recombinant production protocols, can profoundly affect detergent-mediated membrane solubilization<sup>64</sup> and reconstitution.<sup>65</sup> This holds even for short fusion tags, which can have a decisive influence on the success of protein extraction and its modulation by detergents.<sup>66</sup> In correlating protein stability with extraction efficiency, it is important to recall that the choice of reference state is irrelevant as long as it is the same for all detergents and thus cancels out when comparisons are being made.<sup>56</sup> For example, a free-energy difference of  $\sim 10$  kJ/mol between DPC and NG measured for the conformational stability of Mystic (Figure 4a) translates into an equally pronounced advantage in favor of DPC during membrane solubilization, where the common reference state is embodied by the membrane-bound protein instead of the unfolded polypeptide under denaturing conditions. Specifically, strong polar interactions within the protein/detergent complex are required to successfully compete with such interactions in the membrane-embedded state, where zwitterionic and anionic headgroups are abundant. The superior performance of LDAO in selectively extracting Mystic fusion proteins most likely results from a combination of high-affinity headgroup interactions with its poor capability of solubilizing total *E. coli* membrane protein.<sup>67</sup> If the use of LDAO is not an option because of interference with the structural or functional integrity of the target protein, the prime task for optimizing the solubilization of a Mystic-tagged fusion protein thus might consist in trying other, potentially compatible, detergents possessing (zwitter)ionic headgroups (Figure 1b).

## CONCLUSION

Hydrophobicity plays a preeminent role in anchoring nonpolar transmembrane domains of membrane proteins to lipid bilayers. However, some proteins need to associate with lipids yet cannot count on the elaborate cellular machineries required to handle hydrophobic sequences. By establishing conditions enabling reversible equilibrium unfolding experiments on the self-inserting bacterial protein Mystic, we show that stable micelle association can be achieved even for a hydrophilic

membrane protein by virtue of strong interactions with ionic and zwitterionic headgroups abundant in biological membranes. Besides shedding light on a new theme of protein folding and stability at a hydrophobic/hydrophilic interface, these thermodynamic data explain the unusual solubilization behavior of Mystic fusion constructs and thus have implications for the recombinant production of integral membrane proteins.

## METHODS

Mystic DNA from *B. subtilis* was cloned into a pET-30 EK/LIC (Merck, Darmstadt, Germany) expression vector. Recombinant protein production was performed in *E. coli* BL12(DE3) cells at 18 °C. Protein was purified in LDAO by immobilized-metal ion affinity chromatography (IMAC), and the His<sub>6</sub> tag was removed by enterokinase (EK)<sup>68</sup> cleavage. EK and uncleaved fusion protein were removed by reverse IMAC. Detergent was exchanged by anion-exchange chromatography and SEC. A stock solution of 2–3 mg/mL Mystic in buffer (50 mM Tris, 50 mM NaCl, pH 7.4) containing detergent at a concentration 5 mM above its CMC at 8 M urea,  $c_d$ , was diluted to yield solution A (0.25 mg/mL Mystic and  $c_d$  in buffer) and solution B (0.25 mg/mL Mystic and  $c_d$  in urea-containing buffer). Dithiothreitol was added to both solutions to a final concentration of 5 mM. Solutions A and B were mixed to yield 24–48 equally spaced urea concentrations, and samples were allowed to equilibrate for at least 1 h at 20 °C. Data were collected on an automated Chirascapplus CD spectrometer<sup>69</sup> (Applied Photophysics, Leatherhead, U.K.) and an FP-6500 fluorescence spectrometer (Jasco, Groß-Umstadt, Germany) and analyzed by nonlinear least-squares fitting.<sup>70</sup> See Supporting Information for details.

## ASSOCIATED CONTENT

### Supporting Information

Structures and properties of Mystic and detergents used; calorimetric determinations of  $M\beta$ CD dissociation constants and CMC values; additional data on refolding, reversibility, protein/detergent interactions, and aggregation; results of global analyses and detergent statistics in tabular form; supporting discussion; complete materials and methods. This material is available free of charge via the Internet at <http://pubs.acs.org>.

## AUTHOR INFORMATION

### Corresponding Author

mail@sandrokeller.com

### Present Addresses

<sup>‡</sup>J.B.: Department of Biochemistry, University of Toronto, Toronto ON M5S 1A8, Canada.

<sup>§</sup>S.F.: Leslie Dan Faculty of Pharmacy, University of Toronto, Toronto ON M5S 3M2, Canada.

### Author Contributions

<sup>†</sup>These authors contributed equally.

### Notes

The authors declare no competing financial interest.

## ACKNOWLEDGMENTS

We thank Bartholomäus Danielczak, Benjamin Klement, and Martin Textor (all University of Kaiserslautern) for help with protein production; Georg Krainer, Martin Textor, and Dr. Carolyn Vargas (all University of Kaiserslautern) for helpful comments on the manuscript; and Prof. Heiko Heerklotz (University of Toronto) for inspiring discussions. This work was supported by the Leibniz Graduate School of Molecular Biophysics and by the Deutsche Forschungsgemeinschaft (DFG) with grant KE 1478/1-2.

## ■ REFERENCES

- (1) Kyte, J.; Doolittle, R. F. *J. Mol. Biol.* **1982**, *157*, 105.
- (2) White, S. H.; Wimley, W. C. *Annu. Rev. Biophys. Biomol. Struct.* **1999**, *28*, 319.
- (3) Moon, C. P.; Fleming, K. G. *Proc. Natl. Acad. Sci. U.S.A.* **2011**, *108*, 10174.
- (4) Hessa, T.; Kim, H.; Bihlmaier, K.; Lundin, C.; Boekel, J.; Andersson, H.; Nilsson, I.; White, S. H.; von Heijne, G. *Nature* **2005**, *433*, 377.
- (5) Bernsel, A.; Viklund, H.; Falk, J.; Lindahl, E.; von Heijne, G.; Elfsson, A. *Proc. Natl. Acad. Sci. U.S.A.* **2008**, *105*, 7177.
- (6) Cramer, W. A.; Engelman, D. M.; von Heijne, G.; Rees, D. C. *FASEB J.* **1992**, *6*, 3397.
- (7) Therien, A. G.; Grant, F. E.; Deber, C. M. *Nat. Struct. Biol.* **2001**, *8*, 597.
- (8) Ben-Tal, N.; Honig, B.; Miller, C.; McLaughlin, S. *Biophys. J.* **1997**, *73*, 1717.
- (9) Singer, S. J. *Annu. Rev. Biochem.* **1974**, *43*, 805.
- (10) Renthall, R. *Cell. Mol. Life Sci.* **2010**, *67*, 1077.
- (11) Stoddart, D.; Ayub, M.; Höfler, L.; Raychaudhuri, P.; Klingelhofer, J. W.; Maglia, G.; Heron, A.; Bayley, H. *Proc. Natl. Acad. Sci. U.S.A.* **2014**, *111*, 2425.
- (12) Walther, T. H.; Ulrich, A. S. *Curr. Opin. Struct. Biol.* **2014**, *27*, 63.
- (13) Roosild, T. P.; Greenwald, J.; Vega, M.; Castronovo, S.; Riek, R.; Choe, S. *Science* **2005**, *307*, 1317.
- (14) Lundberg, M. E.; Becker, E. C.; Choe, S. *PLoS One* **2013**, *8*, No. e60993.
- (15) Roosild, T. P.; Vega, M.; Castronovo, S.; Choe, S. *BMC Struct. Biol.* **2006**, *6*, 10.
- (16) Kefala, G.; Kwiatkowski, W.; Esquivies, L.; Maslennikov, I.; Choe, S. *J. Struct. Funct. Genomics* **2007**, *8*, 167.
- (17) Liu, X.; Wu, L.; Deng, G.; Li, N.; Chu, X.; Guo, F.; Li, D. *Biochim. Biophys. Acta* **2008**, *1784*, 1742.
- (18) Lee, K. E.; Kim, H. M.; Lee, J.-O.; Jeon, H.; Han, S. S. *Colloids Surf., B* **2008**, *62*, 51.
- (19) Dvir, H.; Choe, S. *Protein Expression Purif.* **2009**, *68*, 28.
- (20) Nekrasova, O. V.; Wulfson, A. N.; Tikhonov, R. V.; Yakimov, S. A.; Simonova, T. N.; Tagvey, A. I.; Dolgikh, D. A.; Ostrovsky, M. A.; Kirpichnikov, M. P. *J. Biotechnol.* **2010**, *147*, 145.
- (21) Petrovskaya, L. E.; Shulgina, A. A.; Bocharova, O. V.; Ermolyuk, Y. S.; Kryukova, E. A.; Chupin, V. V.; Blommers, M. J. J.; Arseniev, A. S.; Kirpichnikov, M. P. *Biochemistry* **2010**, *75*, 881.
- (22) Blain, K. Y.; Kwiatkowski, W.; Choe, S. *Biochemistry* **2010**, *49*, 9089.
- (23) Deniaud, A.; Bernaudat, F.; Frelet-Barrand, A.; Juillan-Binard, C.; Vernet, T.; Rolland, N.; Pebay-Peyroula, E. *Biochim. Biophys. Acta* **2011**, *1808*, 2059.
- (24) Bernaudat, F.; Frelet-Barrand, A.; Pochon, N.; Dementin, S.; Hivin, P.; Boutigny, S.; Rioux, J.-B.; Salvi, D.; Seigneurin-Berny, D.; Richaud, P.; Joyard, J.; Pignol, D.; Sabaty, M.; Desnos, T.; Pebay-Peyroula, E.; Darrouzet, E.; Vernet, T.; Rolland, N. *PLoS One* **2011**, *6*, e29191.
- (25) Choksupmanee, O.; Hodge, K.; Katzenmeier, G.; Chimnarong, S. *Biochemistry* **2012**, *51*, 2840.
- (26) Chowdhury, A.; Feng, R.; Tong, Q.; Zhang, Y.; Xie, X.-Q. *Protein Expression Purif.* **2012**, *83*, 128.
- (27) Lyukmanova, E. N.; Shenkarev, Z. O.; Khabibullina, N. F.; Kulbatskiy, D. S.; Shulepko, M. A.; Petrovskaya, L. E.; Arseniev, A. S.; Dolgikh, D. A.; Kirpichnikov, M. P. *Acta Nat.* **2012**, *4*, 58.
- (28) Marino, J.; Geertsma, E. R.; Zerbe, O. *Biochim. Biophys. Acta* **2012**, *1818*, 3055.
- (29) Xu, Y.; Kong, J.; Kong, W. *Microbiology* **2013**, *159*, 1002.
- (30) Uversky, V. N. *Protein J.* **2009**, *28*, 305.
- (31) Jacso, T.; Franks, W. T.; Rose, H.; Fink, U.; Broecker, J.; Keller, S.; Oschkinat, H.; Reif, B. *Angew. Chem., Int. Ed.* **2012**, *51*, 432.
- (32) Canlas, C. G.; Cui, T.; Li, L.; Xu, Y.; Tang, P. *J. Phys. Chem. B* **2008**, *112*, 14312.
- (33) Debnath, D. K.; Basaiawmoit, R. V.; Nielsen, K. L.; Otzen, D. E. *Protein Eng. Des. Sel.* **2011**, *24*, 89.
- (34) Jacso, T.; Bardiaux, B.; Broecker, J.; Fiedler, S.; Baerwinkel, T.; Mainz, A.; Fink, U.; Vargas, C.; Oschkinat, H.; Keller, S.; Reif, B. *J. Am. Chem. Soc.* **2013**, *135*, 18884.
- (35) Broecker, J.; Keller, S. *Langmuir* **2013**, *29*, 8502.
- (36) Fiedler, S.; Broecker, J.; Keller, S. *Cell. Mol. Life Sci.* **2010**, *67*, 1779–1798.
- (37) Rath, A.; Cunningham, F.; Deber, C. M. *Proc. Natl. Acad. Sci. U.S.A.* **2013**, *110*, 15668.
- (38) Ladokhin, A. S.; Jayasinghe, S.; White, S. H. *Anal. Biochem.* **2000**, *285*, 235.
- (39) Moon, C. P.; Fleming, K. G. *Methods Enzymol.* **2011**, *492*, 189.
- (40) Greene, R. F.; Pace, C. N. *J. Biol. Chem.* **1974**, *249*, 5388.
- (41) Fleming, K. G. *Annu. Rev. Biophys.* **2014**, *43*, 233.
- (42) Hong, H.; Joh, N. H.; Bowie, J. U.; Tamm, L. K. *Methods Enzymol.* **2009**, *455*, 213.
- (43) Booth, P. J. *Curr. Opin. Struct. Biol.* **2012**, *22*, 469.
- (44) Myers, J. K.; Pace, C. N.; Scholtz, J. M. *Protein Sci.* **1995**, *4*, 2138.
- (45) Moon, C. P.; Zaccari, N. R.; Fleming, P. J.; Gessmann, D.; Fleming, K. G. *Proc. Natl. Acad. Sci. U.S.A.* **2013**, *110*, 4285.
- (46) Abel, S.; Lorieu, A.; de Foresta, B.; Dupradeau, F.-Y.; Marchi, M. *Biochim. Biophys. Acta* **2014**, *1838*, 493.
- (47) Hiller, S.; Wider, G.; Imbach, L. L.; Wüthrich, K. *Angew. Chem., Int. Ed.* **2008**, *47*, 977.
- (48) Raman, P.; Cherezov, V.; Caffrey, M. *Cell. Mol. Life Sci.* **2006**, *63*, 36.
- (49) Ben-Tal, N.; Ben-Shaul, a; Nicholls, a; Honig, B. *Biophys. J.* **1996**, *70*, 1803.
- (50) Wimley, W. C.; White, S. H. *Nat. Struct. Biol.* **1996**, *3*, 842.
- (51) Isom, D. G.; Cannon, B. R.; Castañeda, C. A.; Robinson, A.; García-Moreno, B. *Proc. Natl. Acad. Sci. U.S.A.* **2008**, *105*, 17784.
- (52) Dvir, H.; Lundberg, M. E.; Maji, S. K.; Riek, R.; Choe, S. *Protein Sci.* **2009**, *18*, 1564.
- (53) Strickler, S. S.; Gribenko, A. V.; Gribenko, A. V.; Keiffer, T. R.; Tomlinson, J.; Reihle, T.; Loladze, V. V.; Makhatazde, G. I. *Biochemistry* **2006**, *45*, 2761.
- (54) Ben-Naim, A. *Curr. Opin. Colloid Interface Sci.* **2013**, *18*, 502.
- (55) Chong, S.-H.; Ham, S. *Angew. Chem., Int. Ed.* **2014**, *53*, 3961.
- (56) Honig, B. H.; Hubbell, W. L.; Flewelling, R. F. *Annu. Rev. Biophys. Biophys. Chem.* **1986**, *15*, 163.
- (57) Pedro, J. A.; Mora, J. R.; Silva, M.; Fiedler, H. D.; Bunton, C. A.; Nome, F. *Langmuir* **2012**, *28*, 17623.
- (58) Schweighofer, K. J.; Essmann, U.; Berkowitz, M. J. *Phys. Chem. B* **1997**, *101*, 10775.
- (59) Cafiso, D. S. *Curr. Biol.* **1991**, *185*, 185.
- (60) Dewald, A. H.; Hodges, J. C.; Columbus, L. *Biophys. J.* **2011**, *100*, 2131.
- (61) Lomize, A. L.; Pogozheva, I. D.; Lomize, M. A.; Mosberg, H. I. *BMC Struct. Biol.* **2007**, *7*, 44.
- (62) Sansom, M. S. P.; Scott, K. A.; Bond, P. J. *Biochem. Soc. Trans.* **2008**, *36*, 27.
- (63) López, D.; Fischbach, M. A.; Chu, F.; Losick, R.; Kolter, R. *Proc. Natl. Acad. Sci. U.S.A.* **2009**, *106*, 280.
- (64) Maslennikov, I.; Krupa, M.; Dickson, C.; Esquivies, L.; Blain, K.; Kefala, G.; Choe, S.; Kwiatkowski, W. *J. Struct. Funct. Genomics* **2009**, *10*, 25.
- (65) Jahnke, N.; Krylova, O. O.; Hoomann, T.; Vargas, C.; Fiedler, S.; Pohl, P.; Keller, S. *Anal. Chem.* **2014**, *86*, 920.
- (66) Mohanty, A. K.; Wiener, M. C. *Protein Expression Purif.* **2004**, *33*, 311.
- (67) Arachea, B. T.; Sun, Z.; Potente, N.; Malik, R.; Isailovic, D.; Viola, R. E. *Protein Expression Purif.* **2012**, *86*, 12.
- (68) Skala, W.; Goettig, P.; Brandstetter, H. *J. Biotechnol.* **2013**, *168*, 421.
- (69) Fiedler, S.; Cole, L.; Keller, S. *Anal. Chem.* **2013**, *85*, 1868.
- (70) Kemmer, G.; Keller, S. *Nat. Protoc.* **2010**, *5*, 267.